

# A new battery capacity indicator for lithium-ion battery powered electric vehicles using adaptive neuro-fuzzy inference system

K.T. Chau \*, K.C. Wu, C.C. Chan

*Department of Electrical and Electronic Engineering, The University of Hong Kong,  
Pokfulam Road, Hong Kong, Hong Kong*

Received 24 June 2003; accepted 27 September 2003

---

## Abstract

This paper describes a new adaptive neuro-fuzzy inference system (ANFIS) model to estimate accurately the battery residual capacity (BRC) of the lithium-ion (Li-ion) battery for modern electric vehicles (EVs). The key to this model is to adopt newly both the discharged/regenerative capacity distributions and the temperature distributions as the inputs and the state of available capacity (SOAC) as the output, which represents the BRC. Moreover, realistic EV discharge current profiles are newly used to formulate the proposed model. The accuracy of the estimated SOAC obtained from the model is verified by experiments under various EV discharge current profiles.

© 2003 Elsevier Ltd. All rights reserved.

*Keywords:* Adaptive neuro-fuzzy inference system; Battery residual capacity; Electric vehicles; Lithium-ion battery; State of available capacity

---

## 1. Introduction

At the present time and in the foreseeable future, batteries have been agreed to be the major energy source for modern electric vehicles (EVs), including the battery EV (BEV), hybrid EV (HEV) and fuel cell EV (FCEV) [1]. Those viable EV batteries consist of the valve regulated lead acid (VRLA), nickel cadmium (Ni–Cd), nickel zinc (Ni–Zn), nickel metal hydride (Ni–MH), zinc/

---

\* Corresponding author: Tel.: +852-2859-2704; fax: +852-2559-8738.  
E-mail address: ktchau@eee.hku.hk (K.T. Chau).

air (Zn/air), aluminum/air (Al/air), sodium/sulfur (Na/S), sodium/nickel chloride (Na/NiCl<sub>2</sub>), lithium-polymer (Li-polymer) and lithium-ion (Li-ion) types [2].

Recently, it has been identified that those batteries with promising application to EVs are the VRLA, Ni–MH and Li-ion batteries [3]. The VRLA battery is widely accepted for low performance EVs due to its maturity and cost effectiveness; the Ni–MH battery is attractive for moderate performance EVs because of its good specific energy and good specific power; and the Li-ion battery is becoming accepted for high performance EVs because it offers excellent specific energy and excellent specific power. It is anticipated that the Ni–MH battery is an interim battery technology that will be superseded by the Li-ion battery if the initial cost of the Li-ion battery can be significantly reduced upon mass production.

Although the development of EV battery technologies is being actively conducted, the application technology of EV batteries, namely the battery residual capacity (BRC) indicator, cannot catch up with the development pace. The BRC refers to the quantity of electricity remaining in the battery that can be delivered at a certain discharge current and temperature before reaching the specified cutoff voltage. At the fully charged state, the corresponding BRC is denoted the battery available capacity (BAC). Since the BRC estimation is strongly related to the driving range of EVs, an accurate calculation of the BRC is vital. Actually, this technology is the key to commercialization and popularization of EVs.

Starting from the past decade, many battery capacity estimation approaches for the VRLA battery in EVs have been investigated, such as the impedance measurement approach [4] and artificial neural network (ANN) modeling approach [5]. Recently, these approaches have been extended to the Ni–MH battery. For the impedance approach [6], the terminal voltage (response) is measured when a small amplitude ac perturbation (stimulus) is injected into the battery, and hence, the impedance is calculated by the ratio of the response to the stimulus. However, the measured impedance can only indicate the state of charge (SOC), namely the theoretical ratio of the remaining active material to the total active material inside the battery that can be converted into electrical energy from the chemical energy [7], which is actually different from the BRC for EVs. For the ANN modeling approach [8], an ANN model with three layers (input, hidden and output layers) is applied. In the input layer, there are four neurons to represent the battery terminal voltage, discharge current, temperature and discharged capacity. In the hidden layer, five neurons are adopted as a result of a compromise between the estimation accuracy and the complexity of the ANN. In the output layer, there is one neuron indicating the battery capacity. However, this approach does not take into account the influence of the EV discharge current profile, which is essential for accurate estimation of BRC.

Very recently, the ANN modeling approach has been further extended by incorporating fuzzy logic, hence the use of an adaptive neuro-fuzzy inference system (ANFIS) modeling for capacity estimation of the Ni–MH battery [9]. This approach can accurately estimate the state of available capacity (SOAC) of the Ni–MH battery. The SOAC refers to the BRC normalized by the BAC. However, this modeling approach has three shortcomings. First, the discharge currents are always positive, which has not considered the regenerative braking of EVs. Second, the instantaneous temperature, rather than its distributions, is used as an input, which cannot fully describe the influence of temperature. Third, the current profiles are simplified to the climbing hill discharge current, fast discharge current, normal discharge current and small discharge current, which cannot reflect the actual operation of EVs. On the other hand, the use of another

neuro-fuzzy system has been attempted to model the Li-ion battery for estimation of SOC [10]. However, it deals only with constant current discharge profiles, which are far from realistic EV operation.

Since the Li-ion battery is becoming accepted by high performance EVs, such as the Nissan Altra EV, an accurate BRC indicator for Li-ion battery powered EVs is highly desirable. Based on the spirit of our previous work for the Ni–MH battery [9], the purpose of this paper is to propose a new ANFIS model for accurate BRC estimation of the Li-ion battery. Instead of a straightforward extension of our previous work, the model will newly consider the effect of regenerative braking and the use of temperature distributions. Also, rather than using those simplified discharge current profiles, the model will newly employ realistic EV discharge current profiles for both training and validation.

## 2. Li-ion battery characteristics

Since the first announcement of the Li-ion battery in 1991, the Li-ion technology has seen an unprecedented rise to what is now considered to be the most promising rechargeable battery of the future. The Li-ion battery uses a lithiated carbon intercalation material ( $\text{Li}_x\text{C}$ ) for the negative electrode instead of metallic lithium, a lithiated transition metal intercalation oxide ( $\text{Li}_{1-x}\text{M}_y\text{O}_z$ ) for the positive electrode and a liquid organic solution or a solid polymer for the electrolyte. Lithium ions are swinging through the electrolyte between the positive and negative electrodes during discharge and charge. The general electrochemical reactions are described as  $\text{Li}_x\text{C} + \text{Li}_{1-x}\text{M}_y\text{O}_z \leftrightarrow \text{C} + \text{LiM}_y\text{O}_z$ . On discharge, lithium ions are released from the negative electrode, migrate via the electrolyte and are taken up by the positive electrode. On charge, the process is reversed. Possible positive electrode materials are  $\text{Li}_{1-x}\text{CoO}_2$ ,  $\text{Li}_{1-x}\text{NiO}_2$  and  $\text{Li}_{1-x}\text{Mn}_2\text{O}_4$ , which have the advantages of stability in air, high voltage and reversibility for the lithium intercalation reaction.

The  $\text{Li}_x\text{C}/\text{Li}_{1-x}\text{NiO}_2$  type, loosely written as  $\text{C}/\text{LiNiO}_2$  or simply called the nickel based Li-ion battery, generally possesses the cell voltage of 4 V, specific energy of 120 Wh/kg and specific power of 260 W/kg. The cobalt based type has higher specific energy but with a higher cost and an increase of the self discharge rate. The manganese based type has the lowest cost and its specific energy lies between that of the cobalt based and nickel based types. The general advantages of the Li-ion battery are the highest cell voltage (as high as 4 V), excellent specific energy (90–130 Wh/kg), safest design of lithium batteries (absence of metallic lithium) and long cycle life (about 1000 cycles). However, it still suffers from a drawback of high initial cost.

Since the EV driving range highly depends on the BAC, the corresponding influences due to the temperature and discharge current profile are very essential. Instead of using constant current discharge profiles [10] or simplified EV discharge current profiles [9], four realistic EV discharge current profiles are adopted for evaluation. Fig. 1 shows these four profiles, which are based on standard EV driving cycles set by various countries or regions to reflect their EV operations, namely the European driving cycle (ECE), US federal urban driving schedule (FUDS), US federal highway driving schedule (FHDS) and Japan driving mode 10.15 (JM10.15). Notice that the discharge rate is purposely expressed in terms of the *C* rate, rather than in amperes, so as to make the representation more general. For instance, when the nominal capacity of the battery is

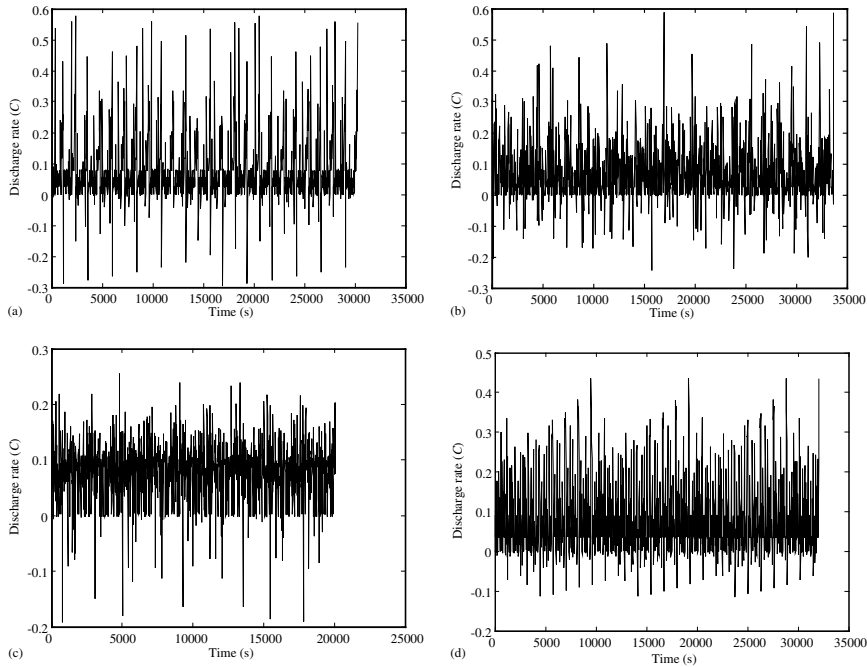


Fig. 1. EV discharge current profiles at 20 °C: (a) ECE; (b) FUDS; (c) FHDS; (d) JM10.15.

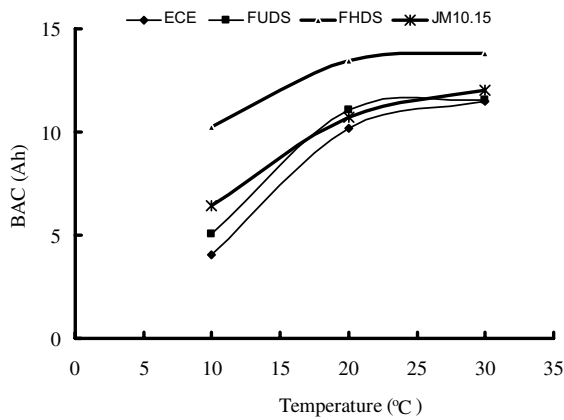


Fig. 2. Comparison of BACs under different temperatures and different EV discharge current profiles.

increased from 15 to 45 A h, the corresponding discharge current is simply enlarged by 3 times, whereas the *C* rate is unchanged.

Based on a commercially available Li-ion battery, Fig. 2 shows the influence of temperature on its BAC under four realistic EV discharge current profiles. It indicates that the BAC remarkably varies with temperature. This temperature sensitivity is much more serious than that of the Ni–MH battery [9], implying that the use of instantaneous temperature as an input of the model for

Table 1  
Comparison of BACs under different EV discharge current profiles at 20 °C

Discharge current profile	BAC (A h)
ECE	10.19
FUDS	11.09
FHDS	13.48
JM10.15	10.71

the Ni–MH battery is insufficient for modeling the Li-ion battery. On the other hand, Table 1 indicates that the influence of various EV discharge current profiles on the BAC at the temperature of 20 °C. From the results in Fig. 2 and Table 1, both the temperature and the discharge current profile should be taken into account during the estimation of SOAC for the Li-ion battery powered EVs.

### 3. Modeling of Li-ion SOAC using ANFIS

#### 3.1. Basic ANFIS architecture

Fig. 3 shows a basic ANFIS architecture [11] in which there are two inputs and one output. In the figure, a circle represents a fixed node, whereas a square denotes an adaptive node. The input parameters are  $x$  and  $y$ . In the first layer, all the nodes are adaptive nodes. The outputs of this layer are the fuzzy membership grades of the inputs, namely  $x$  is fuzzified into  $X_1$  and  $X_2$ , while  $y$  is fuzzified into  $Y_1$  and  $Y_2$ , which can adopt any fuzzy membership function, such as triangular, trapezoidal or bell shaped. In the second layer, the nodes are fixed nodes. They are labeled with  $M$ , indicating that they perform as a simple multiplier. The outputs of this layer are the so-called firing strengths of the rules. In the third layer, the nodes are also fixed nodes. They are labeled with  $N$ , indicating that they play a normalization role to the firing strengths from the previous layer. The outputs of this layer are the so-called normalized firing strengths. In the fourth layer, the nodes are adaptive nodes. The output of each node in this layer is simply the product of the normalized firing strength and the polynomial of input parameters  $f(x, y)$ . In the fifth layer, there

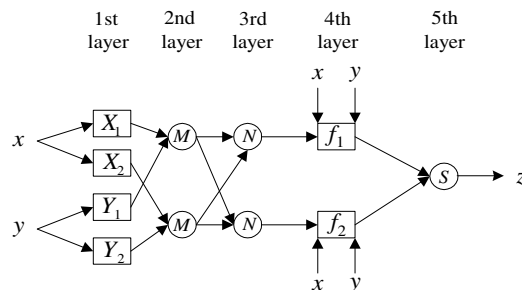


Fig. 3. Basic ANFIS architecture.

is only one single fixed node labeled with  $S$ . This node performs the summation of all incoming signals, hence generating the output  $z$ .

There are two adaptive layers in this ANFIS architecture, namely the first layer and the fourth layer. In the first layer, the modifiable parameters are the so-called premise parameters. In the fourth layer, the modifiable parameters are the so-called consequent parameters. The task of the learning algorithm is to tune all the modifiable parameters to make the ANFIS output match the training data. To improve the rate of convergence, a hybrid algorithm combining the least square method (LSM) and the gradient descent method (GDM) is adopted [12]. The LSM is used to optimize the consequent parameters with the premise parameters fixed. Once the optimal consequent parameters are found, the GDM is used to adjust optimally the premise parameters corresponding to the fuzzy sets in the input domain. The output of the ANFIS is calculated by employing the consequent parameters. The output error is used to adapt the premise parameters by means of a standard back propagation algorithm.

### 3.2. Li-ion SOAC model

The key to the ANFIS model for the BRC estimation of the Li-ion battery is the selection of the output and input parameters. Of course, the output parameter is the desired battery capacity. This capacity can be represented by the SOC, BRC or SOAC. As mentioned before, the SOAC is actually the normalized value of BRC, namely the ratio of BRC to BAC. For EV application, the SOAC with a per unit or percentage value is preferred to the BRC in Watt hours or Joules. The original definition of the SOC is the ratio of the remaining active material to the total active material inside the battery that can be actually converted into electrical energy from the chemical energy. This SOC usually has the same trend as the SOAC but cannot be mathematically related with the SOAC when the discharge current is not fixed. Therefore, in this paper, the SOAC is adopted as the output parameter.

Although the chemical parameters of the battery can directly describe the battery characteristics and capacities, they are impractical to be the input parameters for EV application. From the EV application point of view, the input parameters should be easily measurable and electrically representable, such as the battery terminal voltage, the discharge current, the discharged capacity and the temperature. Previously, the instantaneous battery terminal voltage was chosen as an input parameter for BRC estimation [10]. However, the use of this parameter generally involves the problem of disturbance. Fig. 4 illustrates the relationships between the instantaneous battery terminal voltage and the SOAC under various EV discharge current profiles at the temperature of 20 °C. It can be observed that the battery terminal voltage fluctuates considerably as a result of the EV discharge current variation, whereas the SOAC monotonously decreases with the progress of discharging. These phenomena indicate that the instantaneous battery terminal voltage cannot offer a direct contribution to the SOAC estimation but involves the problem of disturbance, which definitely degrades the estimation accuracy.

To improve the estimation accuracy and to avoid the problem of disturbance, the discharged/regenerative capacity distributions, rather than the instantaneous discharge current, are used as the input parameters. Also, since the temperature sensitivity of the Li-ion battery is significant, the temperature distributions are newly adopted as the input parameters. Notice that the more the divisions of the distributions, the higher is the estimation accuracy but the slower is the con-

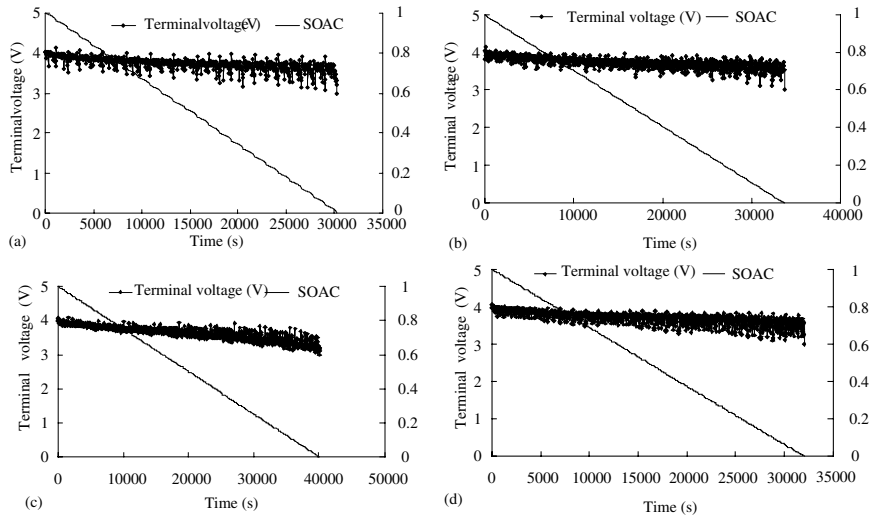


Fig. 4. Effect of instantaneous battery terminal voltage on SOAC under different EV discharge current profiles at 20 °C: (a) ECE; (b) FUDS; (c) FHDS; (d) JM10.15.

vergence. Based on trial and error, the optimal number of input parameters for the BRC estimation of the Li-ion battery is seven, namely four divisions for the discharged capacity, one for the regenerative capacity and two for the temperature. The corresponding input parameters  $X_1(t)$  to  $X_7(t)$  are given by:

- $X_1(t)$ —discharged capacity for  $I_1^l \leq I_d(t) < I_1^u$ ,
- $X_2(t)$ —discharged capacity for  $I_2^l \leq I_d(t) < I_2^u$ ,
- $X_3(t)$ —discharged capacity for  $I_3^l \leq I_d(t) < I_3^u$ ,
- $X_4(t)$ —discharged capacity for  $I_4^l \leq I_d(t) < I_4^u$ ,
- $X_5(t)$ —regenerative capacity,
- $X_6(t)$ —temperature for  $T \geq 20$  °C,
- $X_7(t)$ —temperature for  $T < 20$  °C,

where  $I_d(t)$  is the instantaneous discharge current within four current ranges, namely  $I_i^l$  and  $I_i^u$  ( $i = 1, 2, 3, 4$ ) as listed in Table 2, whereas  $T$  is the temperature within two temperature ranges, namely above 20 °C or not.

Fig. 5 shows the Li-ion model for SOAC estimation using the ANFIS. The seven input parameters, including four discharged capacity distributions, one regenerative capacity and two temperature distributions, are fuzzified into linguistic variables (low and high) as labeled with  $X_i^k(t)$  where  $i = 1, \dots, 7$  and  $k = 1, 2$ . The output of the model is the desired SOAC, which lies between zero and unity. Therefore, the whole process can be viewed as a nonlinear mapping from the input space, consisting of the discharged/regenerative capacity distributions and the temperature distributions, to the output space, namely the SOAC, which represents the BRC of the Li-ion battery.

Table 2

Lower and upper limits of discharge current for discharged capacity distributions

	$i = 1$	$i = 2$	$i = 3$	$i = 4$
$I_i^l$	$0.4C$	$0.27C$	$0.13C$	$0$
$I_i^u$	$0.7C$	$0.4C$	$0.27C$	$0.13C$

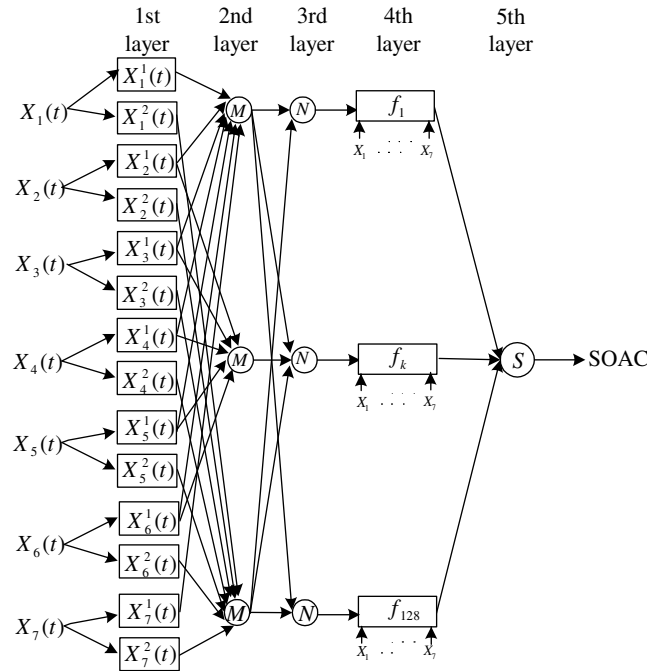


Fig. 5. Li-ion model for SOAC estimation.

**4. Data collection**

A commercially available Li-ion battery is used for experimentation. This battery has the nominal voltage of 3.6 V and the nominal capacity of 15 Ah at the discharge rate of 0.2C. This nominal capacity is just a reference value, since the actual discharge rate in an EV is usually much larger than 0.2C. As mentioned before, the BAC is defined as the quantity of electricity at the fully charged state that can be delivered at a certain discharge current profile and temperature till the specified cutoff voltage of 3 V is reached.

As shown in Fig. 6, the system setup for experimentation is the Digatron Battery Testing System BTS-600, which consists of four main parts:

- A programmable charger in which various charging algorithms, including constant voltage charging, constant current charging, multistage variable voltage variable current charging and pulse charging, can be performed.



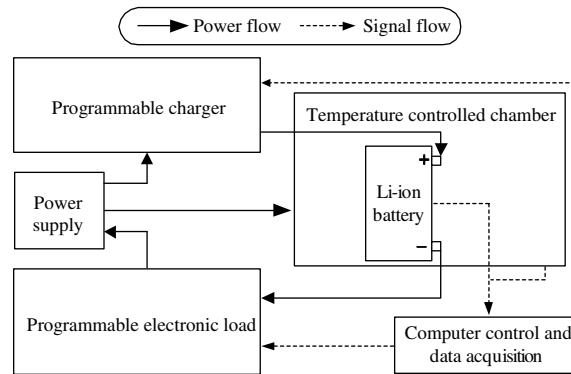


Fig. 6. Battery testing system for data collection.

- A programmable electronic load in which various discharging algorithms, including constant current discharge, varying current discharge and EV discharge current profiles, can be performed.
- A temperature controlled chamber in which the battery can be tested under any predefined air temperature ranging from  $-20$  to  $50$  °C.
- A computer control and data acquisition system in which control signals are generated to feed the programmable charger and the programmable electronic load, while all necessary experimental data are automatically acquired.

A series of experiments need to be conducted for data collection. These experiments are based on the realistic EV discharge current profiles, namely the ECE, FUDS, FHDS and JM10.15, under different temperatures, namely 10, 20 and 30 °C. The experimental data are automatically recorded and tabulated, with each row of data containing the terminal voltage, the discharge current, the temperature, the discharged/regenerative capacity and the SOAC.

## 5. Model training and validation

The data collected from the aforementioned experiments are separately used to train and validate the proposed SOAC model. The whole data set is composed of 12 data files obtained from 12 tests. It is then divided into two separate data sets, the training data set and the validation data set. The training data set is used to train the SOAC model, whereas the validation data set is used to validate the accuracy and effectiveness of the trained model for SOAC estimation.

To assess the accuracy of the proposed model, the average percentage error (APE) of the SOAC is adopted for evaluation. This APE is defined as the average of the percentage errors between the actual SOACs obtained from experiments and the estimated SOACs obtained from the trained model. The APEs for both the training data set and the validation data set are calculated.

Firstly, based on the training data set, the relationship between the estimated SOAC and the actual SOAC is shown in Fig. 7. As expected, the agreement is excellent, and the corresponding APE is only of 0.16%.

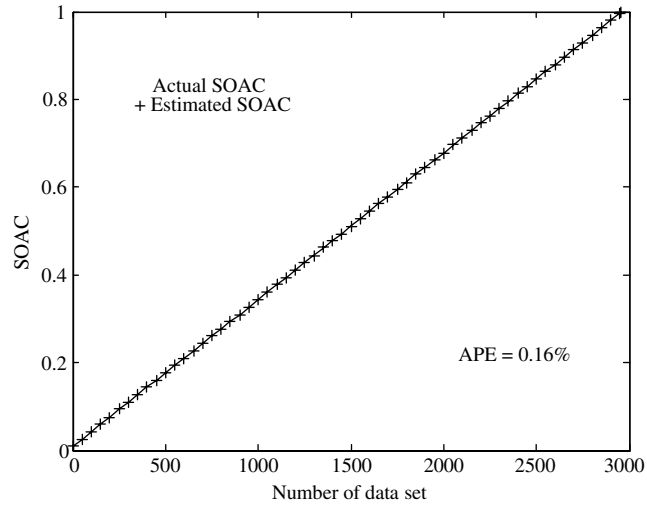


Fig. 7. Comparison between actual SOAC and estimated SOAC for training data.

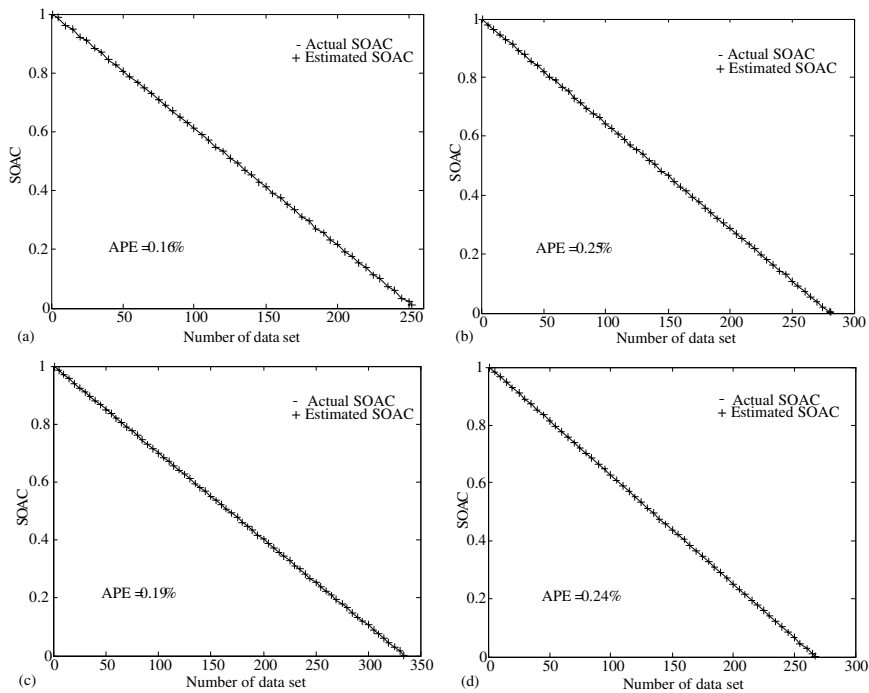


Fig. 8. Comparison between actual SOAC and estimated SOAC for validation data under different EV discharge current profiles at 20 °C: (a) ECE; (b) FUDS; (c) FHDS; (d) JM10.15.

Secondly, based on the validation data set, the accuracy of the trained model is assessed. Fig. 8 shows the relationships between the estimated SOAC and the actual SOAC under the ECE,

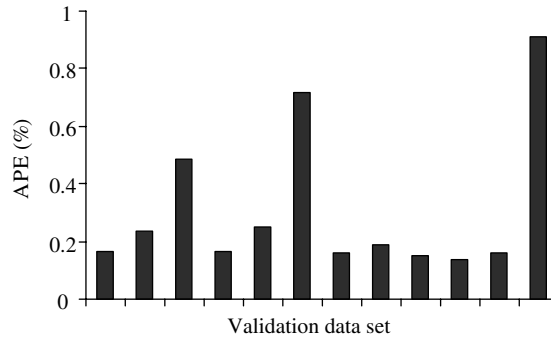


Fig. 9. APEs of all 12 validation data sets.

FUDS, FHDS and JM10.15 operations at the temperature of 20 °C. These comparisons confirm that the proposed model provides a highly accurate estimation of the SOAC for the different operating profiles of EVs. Fig. 9 summarizes that the APEs of all 12 validation data sets are within 1%, which is significantly better than the 5.5% in Ref. [10] or the 2.7% in Ref. [9].

### 6. Model realization

The proposed SOAC model can be easily realized as a practical BRC indicator by using a low cost microcontroller. Fig. 10 shows the corresponding diagram of realization. The major hardware of this indicator is a microcontroller, such as the Intel 80C196, which incorporates all necessary functions including A/D conversion of a single chip microcomputer. The software of this indicator mainly consists of three components, namely the classification unit, the integration unit and the ANFIS unit. The classification unit is to categorize the discharge current into the four predefined current ranges, to identify the regenerative current and to classify the temperature into the predefined two temperature ranges. The integration unit is to integrate the discharged/regenerative currents and, hence, to produce the discharged/regenerative capacity distributions. The ANFIS unit is finally to make an estimation of the SOAC by using the proposed model. Evidently, the assembly language embedded in the microcontroller can realize all these functions.

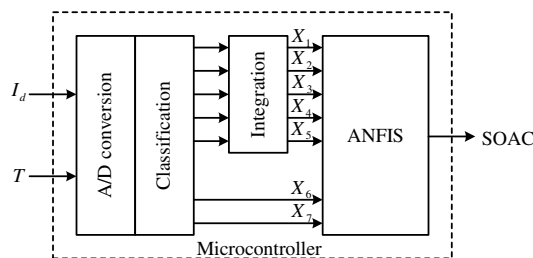


Fig. 10. Realization of proposed model.

## 7. Conclusions

This paper has presented a new SOAC model to estimate accurately the BRC of the Li-ion battery for modern EVs. The key to this model is to adopt newly both the discharged/regenerative capacity distributions and the temperature distributions as the input parameters and the SOAC as the output parameter. Moreover, realistic EV discharge current profiles are newly used to formulate the proposed model. By comparing the estimated SOACs obtained from the model and the actual SOACs obtained from experiments, the proposed model is validated to offer a high accuracy.

## Acknowledgements

The work was supported by the Committee for Research and Conference Grants of the University of Hong Kong.

## References

- [1] Chan CC, Chau KT. *Modern electric vehicle technology*. Oxford: Oxford University Press; 2001.
- [2] Chau KT, Wong YS, Chan CC. An overview of energy sources for electric vehicles. *Energy Convers Manage* 1999;40(10):1021–39.
- [3] Chau KT, Wong YS. Hybridization of energy sources in electric vehicles. *Energy Convers Manage* 2001;42(9):1059–69.
- [4] Karden E, Mauracher P, Schoepe F. Electrochemical modeling of lead-acid batteries under operating conditions of electric vehicles. *J Power Sources* 1997;64(1):175–80.
- [5] Shen WX, Chan CC, Lo EWC, Chau KT. A new battery available capacity indicator for electric vehicles using neural network. *Energy Convers Manage* 2002;43(6):817–26.
- [6] Bundy K, Karlsson M, Lindbergh G, Lundqvist A. An electrochemical impedance spectroscopy method for prediction of state of charge of a nickel-metal hydride battery at open circuit and during discharge. *J Power Sources* 1998;72(2):118–25.
- [7] Aylor JH, Thieme A, Johnson BW. A battery state of charge indicator for electric wheelchairs. *IEEE Trans Indust Electron* 1992;39(5):398–409.
- [8] Peng JC, Chen YB, Eberhart R, Lee HH. Adaptive battery state of charge estimation using neural network. In: *Proceedings of International Electric Vehicle Symposium, 2000, CD-ROM*.
- [9] Chau KT, Wu KC, Chan CC, Shen WX. A new battery capacity indicator for nickel-metal hydride battery powered electric vehicles using adaptive neuro-fuzzy inference system. *Energy Convers Manage* 2003;44:2059–71.
- [10] Lee YS, Wang J, Kuo TY. Lithium-ion battery model and fuzzy neural approach for estimating battery state-of-charge. In: *Proceedings of International Electric Vehicle Symposium, 2002, CD-ROM*.
- [11] Jang JSR, Sun CT, Mizutani E. *Neuro-fuzzy and soft computing: a computational approach to learning and machine intelligence*. NJ: Prentice-Hall; 1997.
- [12] Jang JSR. ANFIS: Adaptive-network-based fuzzy inference system. *IEEE Trans Syst, Man Cybernet* 1993;23(3):665–85.